Hindawi
Journal of Electrical and Computer Engineering
Volume 2023, Article ID 8643537, 14 pages
https://doi.org/10.1155/2023/8643537

Research Article

Key Transmission Section Search Based on Graph Theory and PMU Data for Vulnerable Line Identification in Power System

Miao Yu[1,2] **Shouzhi Zhang**[1] **Fang Shi**[3] **Jianqun Sun**[1] **Jingjing Wei**[1] **Yixiao Wu**[1] **and Jingxuan Hu**[1]

[1]*School of Mechanical-Electronic and Vehicle Engineering, Beijing University of Civil Engineering and Architecture, Beijing 100044, China*
[2]*Beijing Engineering Research Center for Building Safety Inspection, Beijing 100044, China*
[3]*School of Electrical Engineering, Shandong University, Jinan 250061, China*

Correspondence should be addressed to Miao Yu; olivermiaoer@163.com

Received 7 August 2023; Revised 4 October 2023; Accepted 16 October 2023; Published 30 October 2023

Academic Editor: Kusum Verma

Failure of vulnerable lines in the power system often results in tidal shifts, and triggering chain failures and their corresponding transmission sections are concentrated manifestations of the weak links in the power system. It is very important to identify the vulnerable lines and search the transmission section to prevent the chain faults as well as to analyze the stability of the power system. Aiming at the problems of inaccurate search of vulnerable lines, difficulties adapting to the complex and changing power system as well as wrong selection and omission of transmission section search in the existing references, this paper proposes an algorithm for searching vulnerable lines and their key transmission sections based on the graph theory and PMU (phasor measurement unit) data. First, the method combines with the graph theory and PMU data to construct the grid topology map. Second, the comprehensive indicators for screening vulnerable lines are proposed by fully considering the network topology and line capacity, which combines with power exchange efficiency and energy fluctuation probability. Third, the distance matrix in the Floyd algorithm is transformed into a unit group that can store more elements, which reduces the traversal times of the algorithm and improves computational efficiency. The fast localization of transmission cross sections associated with vulnerable lines is realized. Finally, the critical transmission cross sections are screened according to the line outage distribution factor and line safety margin. The IEEE 39-bus system is selected for simulation experiments, and the simulation results show that the key transmission section search method proposed in this paper can better adapt to the variable power grid and is faster and more accurate than the other common method.

1. Introduction

Large-scale power outages have been occurring time and again, causing severe economic losses. For example, the 2012 Indian blackout affected more than 600 million people [1]. As recorded in reference [2], it was mentioned that a huge blackout occurred in Brazil when two transmission lines failed and tripped due to a mountain fire, resulting in the unraveling of the Far Northwest grid. A large proportion of such accidents were due to the tripping or disconnection of lines in the grid due to faults. As soon as a fault occurred, the protective device removed the component in question, while the current of the component was diverted to the transmission line of high correlation, leading to a chain of failures [3, 4]. In addition, the disconnection of heavy-loaded lines in the grid could also cause the current to be shifted, thus causing a chain fault. And each event in the chain of failures further weakened the power system which led to a complete grid blackout [5, 6].

Vulnerable lines in the grid are the links in the network transmission that need to be focused on. The key transmission section is a weak transmission link formed by the

current transfer caused by the failure of the vulnerable lines. It is very important to quickly and accurately locate the vulnerable lines and their key transmission sections in the complex power grid. In the past, the identification of vulnerable lines was often a single consideration, and the determination of the transmission section could not be adapted to the development of variable power grids [7–12]. And the current power grid is developing towards digitalization and intelligence, so it is necessary to propose a data-driven fast identification method for transmission sections.

Taking DC modeling analysis as an example, researchers have proposed a variety of vulnerable line assessment methods, which can be roughly divided into two categories. One is the analysis method based on the network structure. For example, reference [7] considered the correlation between interconnected control regions decoupled by the Schur complement matrix and applied the regional decomposition method to decentralize the calculation of the total transmission capacity of the power system. As mentioned in reference [8], a multiregion line transmission calculation method based on the network decomposition method of REI (radial, equivalent, and independent)-type network equivalents was proposed, in which each region could use the REI equivalents of the external regions to calculate its total transmission capacity by continuous power flow. The other one analyzed the load from the line itself. For example, reference [9] used a DC distribution factor to calculate the thermal limit of the line and assess the line transfer capability. However, the accuracy of a single evaluation metric for an increasingly complex grid needed to be tested.

The transmission section mainly reflects the problems that occur after the occurrence of interlocking faults. Relevant researchers generally consider two aspects when solving such problems. One is the structural problem represented by topological complementary graphs. For example, a Markov tree-based chained fault assessment method was proposed in reference [10]. This type of approach tended to ignore the effect of line capacity on the results. The other one analyzed the impact of the current transfer due to faulty elements. Similarly, reference [11] identified system instability by analyzing the transfer of electrical quantities in the critical section and thus obtaining the concavity and convexity of the disturbed phase trajectory of the AC critical branch. And reference [12] screened out the critical transmission section by establishing the correlation matrix of faulty elements and tidal current transfer channels based on the open-break distribution factor. However, they all required high-level and time-consuming algorithm calculation, and the regional information under the decentralized framework could not be fully accessed, which would inevitably affect the objectivity of the assessment results.

Graph theoretic methods are generally applied to solve topological problems. And facing the complex power grid structure, researchers have applied their knowledge of graph theory to simplify it topologically. A series of related studies have been further developed. For example, in the assessment of vulnerable lines in power grids, reference [13] analyzed the vulnerability of lines from the aspects of power transmission capacity and load capacity of power grids by using the topological complementary characteristics of the network to find the electrical gaps between the nodes. Reference [14] proposed a cascading fault model based on the theory of complex networks, which could intuitively reflect the resistance to damage of the high-risk nodes in the power grid. On the basis of which, reference [15] proposed a vulnerable transmission line identification method using K-shell decomposition depth, which fully took into account the dynamic characteristics of the grid and the postfault transmission capability. Reference [16] assessed the transmission network vulnerability by converting the grid with spatial information into a fault propagation map with temporal information. Reference [17] added entropy and Spearman rank correlation coefficients through a multimetric decision-making method based on interconditional correlation, which could accurately identify the important transmission lines with topological characteristics of complex networks by utilizing the topological characteristics of complex networks. However, this kind of research still stayed in the first-level network structure. Thus, reference [18] proposed a weighted index applied to the second-level correlation network to realize the identification of vulnerable lines in the power grid. The use of graph-theoretic methods avoided errors caused by regional conditions and greatly reduced the computational burden.

For the search of transmission sections that are susceptible to the influence of the tidal shifts occurring in the vulnerable lines under chained faults, the application of graph theory methods not only improves the accuracy of the results, but more importantly, it is able to reflect the line association. For example, reference [19] proposed a fast search and identification method for weak transmission sections based on the automatic subnetwork combination technique, which automatically combined the subnets with a more intuitive expression of their structural associations. In order to further shorten the computation time and fully consider multiple topological complementary changes, reference [20] utilized a cut-set search algorithm based on graph-theoretic matrix operations and used security margins to quickly identify typical transmission sections in the grid. Reference [21] combined a key section identification method with multi-fault disturbances and a weak section identification method after multi-faults induced topological changes to analyze multiple types of lines. A key transmission section identification method considering multiple predicted faults was proposed. Reference [22] accessed the weighted network topology in an AC current model to identify critical sections in the grid using complex network centrality theory as well as line net capacity and vulnerability indicators. Reference [23] transformed complex grids into their dual graphs, utilized the improved structural hole theory and M-Burt method to rank the vulnerability of transmission lines, and designed a cascading mitigation strategy that took into account vulnerable transmission lines. Such methods simplify the tedious steps of computation and also make the correlation between lines more explicit. The above methods avoid the drawbacks of real network partitioning and the loss of information in

a decentralized framework. However, they do not capture the characteristics of the new power system, thus failing to achieve timely monitoring of the grid.

Synthesizing the shortcomings of previous literature, this paper proposes a transmission section search method based on graph theory and PMU data. The main contributions of this paper are as follows.

(1) Aiming at the single aspect considered in the previous evaluation indicator for vulnerable lines, a comprehensive evaluation indicator for vulnerable transmission lines is proposed. The indicator fully considers the system structure and the carrying capacity of the line itself and can more comprehensively and accurately assess the condition of the line.

(2) The problems of wrong selection, omission, and long calculation time exist in the search for key transmission sections. In this paper, the Floyd algorithm is improved to improve its calculation accuracy and efficiency, which can realize an accurate and fast search of the transmission section.

(3) According to the results of transmission section identification, combined with the line outage distribution factor and line safety margin indicator, the determination of key transmission sections is completed.

The rest of this paper is organized as follows. Section 2 presents the construction of power grid topology and the definition of line weight. Section 3 first introduces the vulnerability line identification method and proposes the comprehensive vulnerability determination indicator test method. Then, the search method for the first k minimum weight path is proposed. Finally, the method of searching the key transmission section is proposed. In Section 4, an IEEE 39-bus system is selected for experimental simulation, and the comparison of the operating time between the proposed method and the traditional method is given. Section 5 summarizes.

2. Network Model and Identification Indicators

2.1. Graph Theory and Model. The cascading failure of power systems can be studied by using the topology of complex power grids. The topology diagram can directly reflect the coupling relationship of power systems. This paper mainly uses similarity theory to construct the topological graph. This will facilitate the use of spatial weighting ideas to assign weights to lines. This will facilitate the use of spatial weighting ideas to assign weights to lines. This process greatly preserves the structural characteristics of the original network and provides convenience for subsequent calculations. Considering the structural characteristics of the power grid and the status characteristics of the line, the topological map is constructed as shown in Algorithm 1.

As shown in Figure 1, this paper uses IEEE 9-bus to illustrate. Layer A represents the original network structure, and layer B reflects the topological relationship. The node in B is the location of the line in A, and it is also the location of PMU data.

The spatial weighting matrix C can be interpreted as a network that contains connections between measurement points and PMUs, and it also contains an observation [24]. Matrix C is a pairwise Euclidean distance coefficient c_{ij} that reflects the relationship between nodes. Matrix C is denoted as follows:

$$C = \left[c_{ij}\right] = \begin{cases} c_{ij} = \min p_{ij}, & i \neq j, \\ 0, & i = j, \end{cases} \tag{1}$$

where c_{ij} and p_{ij} are the distance and the shortest path from node i to node j, respectively. Generally, the values in C are normalized so that the range is 0~1.

Similarity matrix S can be defined as follows [25]:

$$s_{ij} = 1 - \left(\frac{c_{ij}}{\max c_{ij}}\right)^2 = 1 + \left(\frac{d_{ij}}{\max d_{ij}}\right)^2, \tag{2}$$

and

$$S = \left[s_{ij}\right] = l_n l_n^T - \frac{C^*}{\max\left(c_{ij}^*\right)^2}, \tag{3}$$

where $c_{ij}^* = (d_{ij})^2$. d_{ij} is the similarity between lines. l_n is the n-dimensional vector of all elements 1. The superscript T represents the transpose. The value range of the similarity coefficient s_{ij} is from 0 to 1. The larger the value s_{ij} is, the higher the mild connection will be.

2.2. Line Weight. Let $[x_1, x_2, \ldots, x_m]$ denote a set of system voltage data measured at position $[1, 2, \ldots, m]$, and let x_i denote unknown data at unmonitored position x_i in a study area, as shown in Figure 2. The location of PMUs is random. Then, when a set of measurement data is given at time t_j, the estimated value x_i of a random process of an unobserved part of $\hat{x}_i(t)$ can be obtained by the weighted average of sampling points [26].

$$\hat{x}_i(t) = \sum_{l=1}^{m} \omega_{il} x_l\left(t_j\right) = \sum_{l=1}^{m} \omega_{il} \sum_{k=1}^{p} a_k(t)\varphi_k(x). \tag{4}$$

In (4), i is the estimated position. l is the sensor position. m is the number of PMUs around the measurement value that affects the position i. ω_{il} is the unknown prediction weight between the measurement point l and the sampling point i.

Input: Grid Node Information
(1) Obtain spatial weighted matrix C.
(2) Construct the nonweighted graph.
(3) Normalize the value in matrix C.
(4) Convert to a similarity matrix S. The value in matrix S represents the grid connection strength.
(5) Give the topology weight.

Algorithm 1: Construction of power system topography.

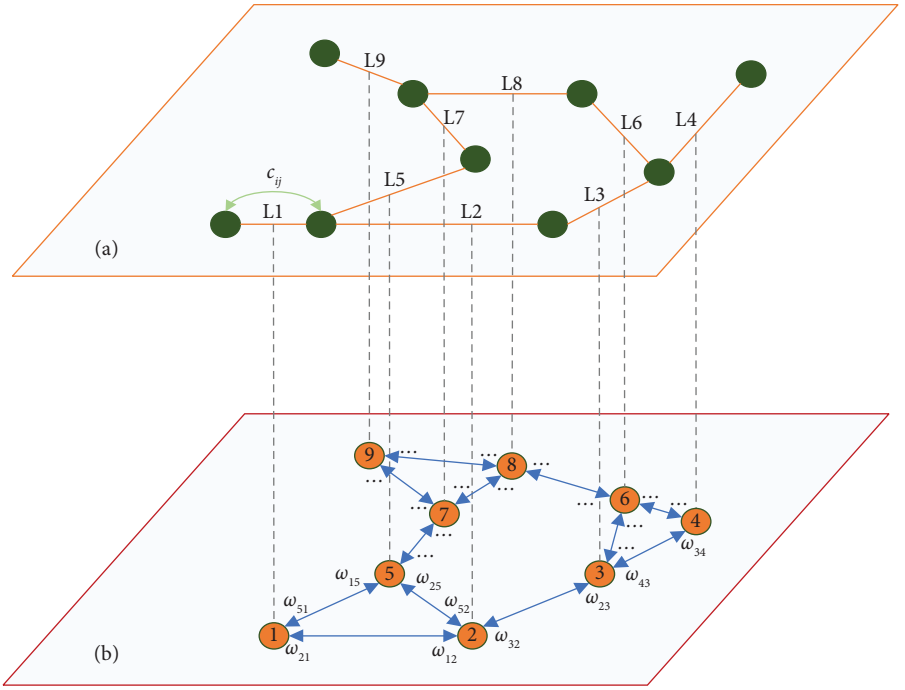

Figure 1: IEEE 9-bus topology network case.

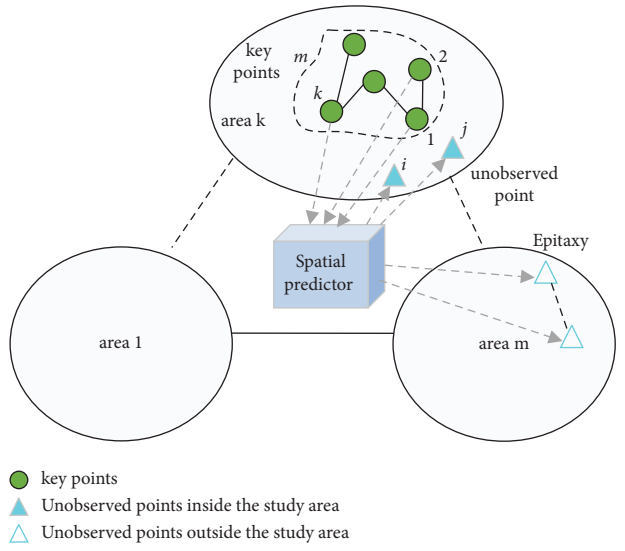

Figure 2: Example of a monitoring system.

Weights can be divided into two categories, including realistic physical weights represented by electrical distances and abstract weights described by conductance ratios to represent the strength of the line interaction. This paper is based on the latter weight selection; it is more in line with this article for vulnerable lines related to the key transmission section search requirements. When studying the actual power grid and considering the multidimensionality of the network structure, the concept of spatial similarity can be used to represent the degree of interaction between lines; then, the weight ω_{il} between the monitoring point l and the sampling point i can be defined as follows [27]:

$$\begin{aligned}\omega(x_i, x_l) &= \omega_{il} \\ &= \frac{s(x_i, x_l)}{\sum_{l=1}^{m} s(x_i, x_l)},\end{aligned} \tag{5}$$

and

$$\omega_{ij} = \sum_{k=1}^{p} \varphi_{ik}(x)^T a_{ik}(t), \tag{6}$$

where $s(x_i, x_l)$ is a similarity coefficient based on a set of measurements, which is used to quantify the similarity between site i and site l. a_{ik} is a set of changing temporal patterns; φ_{ik} is an orthonormal basis vector describing the spatial structure of these patterns.

After calculating the weights, the system behavior estimate for the unsampled points can be calculated according to (4), such as

$$\begin{bmatrix} \widehat{x}_1(t) \\ \widehat{x}_2(t) \\ \vdots \\ \widehat{x}_m(t) \end{bmatrix} = \begin{bmatrix} \omega_{11} & \omega_{12} & \cdots & \omega_{1p} \\ \omega_{21} & \omega_{22} & \cdots & \omega_{2p} \\ \vdots & \vdots & \vdots & \vdots \\ \omega_{m1} & \omega_{m2} & \cdots & \omega_{mp} \end{bmatrix} \begin{bmatrix} \sum_{k=1}^{p} \varphi_{ik}(x)^T a_{1k}(t) \\ \sum_{k=1}^{p} \varphi_{ik}(x)^T a_{2k}(t) \\ \vdots \\ \sum_{k=1}^{p} \varphi_{ik}(x)^T a_{pk}(t) \end{bmatrix}. \tag{7}$$

3. Key Transmission Section Search

3.1. Power Exchange Efficiency. The power transmission distribution factor (PTDF) in the power grid reflects the influence of power variation between nodes on other lines. Applying PTDF to the topology structure diagram can reflect the relationship between the mapped lines. The performance of the topology graph greatly retains the characteristics of the original network, which facilitates us to analyze the line relationship of the original grid from the perspective of structure. The flow direction in long-distance high-voltage transmission lines can be approximated as a DC distribution. This is because the phase difference between the nodes is very small, and the branch reactance value x_{ij} is much larger than the resistance value r_{ij}. So, PTDF can be calculated as follows:

$$\begin{aligned}\lambda_{ij}^{lm} &= \frac{\Delta P_{ij}}{\Delta P_{km}} \\ &= \frac{X_{ik} - X_{im} - X_{jk} + X_{jm}}{x_{ij}},\end{aligned} \tag{8}$$

where ΔP_{km} and ΔP_{ij} are the amounts of power variation from the supply point v_k to the load point v_m, and on the line l_{ij} under the influence of ΔP_{km}, respectively. X_{jk} is the element in the reactance matrix.

The PTDF quantifies the power transfer of the branch circuit between the supply nodes and load nodes and reflects the degree of association between node pairs. The line vulnerability can be evaluated according to the PTDF modulus, which can be calculated by the PTDF matrix M_{PTDF}.

$$M_{\mathrm{PTDF}} = \begin{bmatrix} |\lambda_{11}| & |\lambda_{12}| & \cdots & |\lambda_{1n}| \\ |\lambda_{21}| & |\lambda_{22}| & \cdots & |\lambda_{2n}| \\ \vdots & \vdots & \ddots & \vdots \\ |\lambda_{m1}| & |\lambda_{m2}| & \cdots & |\lambda_{mn}| \end{bmatrix}. \tag{9}$$

The total power exchange efficiency $\varsigma(i, j)$ of the lines is expressed as follows:

$$\varsigma(i, j) = \frac{\sum_{i \in m, t \in n} |\lambda_{i,t}(i, j)|}{m}. \tag{10}$$

The $\varsigma(i, j)$ value of the line is positively correlated with the criticality of the line. The proposed power exchange efficiency is analyzed using the node reactance matrix. The topological nodes reflect the line characteristics of the original network, which means that the analysis does not involve the influence of power flow propagation. This will improve the stability of parameter analysis.

3.2. Tidal Transfer Entropy Analyzed from the Energy Perspective. This section mainly introduces the tidal transfer entropy. Different from the traditional transfer entropy, it is considered from the perspective of energy. The main voltage parameters are directly measured by PMUs at a sampling rate of 0.02 s. When the transmission system is faced with high penetration of renewable energy generation, the initial power flow of the system needs to be updated with the current situation. Figure 3 shows the model diagram of the acquisition system. The voltage matrix $A(t)$ measured by PMU can be obtained directly from the system. Each element in the voltage matrix is the voltage measurement value of the PMU at a certain time node. The number of PMUs is selected to cover each power grid line; that is, matrix $A(t)$ can be regarded as a data network map, which is defined as follows:

$$\begin{aligned}A(t) &= \begin{bmatrix} \mathbf{a}_1(t) \\ \mathbf{a}_2(t) \\ \vdots \\ \mathbf{a}_m(t) \end{bmatrix} \\ &= \begin{bmatrix} a_{11}(t) & a_{12}(t) & \cdots & a_{1n}(t) \\ a_{21}(t) & a_{22}(t) & \cdots & a_{2n}(t) \\ \vdots & \vdots & \ddots & \vdots \\ a_{m1}(t) & a_{m2}(t) & \cdots & a_{mn}(t) \end{bmatrix},\end{aligned} \tag{11}$$

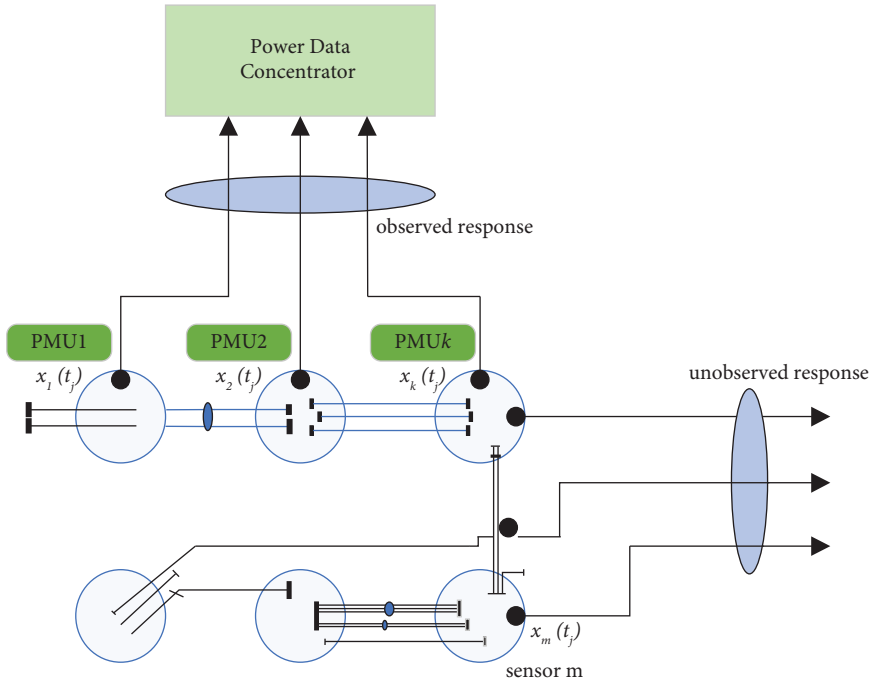

Figure 3: Acquisition system model diagram.

where $\mathbf{a}_k(t) = [a_{k1}(t), a_{k2}(t), \ldots, a_{kn}(t)], k = 1, 2, \ldots, m$.

For a certain time t, the energy of the line is defined as follows:

$$E(t) = \sum_{k=1}^{m} \mathbf{a}_k^T(t)\mathbf{a}_k(t) = \sum_{k=1}^{m} E_k(t). \tag{12}$$

After obtaining the energy of the line, in order to intuitively reflect the results of parameter comparison, the energy fluctuation probability $p_k(t)$ of the evaluation indicator is proposed. It is the proportion of the total energy of the line in a certain period of time in the total energy of the system, which can be calculated by the following formula (13):

$$p_k(t) = \frac{E_k(t)}{\sum_{k=1}^{m} E_k(t)}. \tag{13}$$

The average energy fluctuation probability is further calculated, and the lines larger than this indicator will be defined as the lines that should be focused on.

$$p_{\text{ave}}(t) = \frac{E_{\text{ave}}(t)}{\sum_{k=1}^{m} E_k(t)}. \tag{14}$$

The greater the value of $p_k(t)$, the greater the line load, and the more vulnerable to the negative impact of power flow will transfer. It is worth noting that $p_k(t)$ is a dynamic indicator, and its value changes with the real-time measurement results of PMUs.

3.3. Comprehensive Judgment Indicator of Line Vulnerability. When assessing the vulnerability of the system line, a single aspect of the analysis is not reliable. In this paper, the comprehensive evaluation indicator Γ_{ij} of line vulnerability is proposed based on the above two indicators [28]. It is considered from two aspects: structure and power tidal, and more in line with the actual grid operation.

$$\Gamma_{ij} = \alpha\varsigma(i, j) + (1 - \alpha)p_k. \tag{15}$$

In (15), α is a weight coefficient that balances the relationship between complex grid structures and line flow impacts.

3.4. Flow Transfer Section Search Based on the Floyd Algorithm. The simple work on the identification of vulnerable transmission lines in the power grid has been discussed in detail by us in reference [28]. For further study, the main topic of this paper is how to search for the set of transmission lines that are susceptible to the shifting of the developing currents after the failure of vulnerable lines, which can be helped by the Floyd algorithm. Therefore, the research questions and motivations of the two papers are quite different. The traditional Floyd algorithm is used to search for the shortest line between two points. Its computational complexity is low, and the computation time has certain superiority. In this paper, the Floyd algorithm is improved, and the spatial similarity is used as the weight to weigh the line topology graph. Searching for the first k minimum weight path of the power grid is to find the power flow transfer section of the system. The improved algorithm can store all the power flow-influencing lines. The improvement of the Floyd algorithm based on the graph theory

method mentioned above ensures that the flow section corresponding to each vulnerable line can be well selected. In addition, the overall computation time of the algorithm has also been greatly improved. The specific steps are shown in Algorithm 2.

For Step 2, assuming that there is no negative weight loop, the diagonal elements of the weight matrix W are all 0. If $k = i$ or j, $W_{ik} + W_{ki} = W_{ij}$ is constant. If $\omega_{ij} = \infty$ is not ruled out, then $W_{ik} + W_{ki} \equiv W_{ij} \equiv \infty$. This holds for any equality and adds all k to the set without getting the desired result.

Note that for Step 3 and Step 4, as shown in Figure 4. If $W_{ik} + W_{ki} < W_{ij}$ occurs, let $W_{ij} = W_{ik} + W_{ki}$ and update the distance matrix to $R(i, j) = R(i, k)$. For $W_{ik} + W_{ki} = W_{ij}$, their weights are the same, so just update the routing matrix R. The resulting R is a unit group rather than a matrix, and the corresponding matrix changes are shown in Figure 5.

For Step 10, the number of elements in the first traversal unit group is denoted as ①, and the number of elements in the second traversal unit group is denoted as ②. According to this analogy, and until the end of the traversal, the shortest path number is ① × ② ×. . .

3.5. Key Transmission Section Screening. To judge whether the power flow transfer section is a key section, the influence degree of any branch disconnection on the remaining lines should be considered. Overloads or fault lines in power system are prone to power flow transfer and cascading failure when they are cut off. For line l, its active power can be calculated as follows:

$$\Delta P_k^l = D_{k-l} P_l, \tag{16}$$

where P_l is the power before breaking; ΔP_k^l is the power variation after breaking; and D_{k-l} is the line outage distribution factor and it is used to measure the proportion of line power flow transfer. D_{k-l} can directly reflect the influence degree of power flow between lines. The greater its value, the more serious the impact. Its calculation formula is in reference [29].

$$\begin{aligned} D_{k-l} &= \frac{X_{k-l}/x_k}{1 - X_{l-l}/x_l}, \\ X_{k-l} &= M_k^T X M_l, \\ X_{l-l} &= M_l^T X M_l, \end{aligned} \tag{17}$$

where X_{k-l} is the mutual impedance between node k and node l, and X_{l-l} is the self-impedance of node l. x_k and x_l are the elements of the reactance matrix X, which represents the reactance value of the line. M_k and M_l are the correlation matrices of the node.

To filter out branches with a great influence on power flow and obtain the LODF transmission section, the threshold is set to filter out the branches larger than the threshold in the first k minimum weight path.

$$D_{k-l} > D_{\text{set}}. \tag{18}$$

The value of D_{set} is generally set according to expert experience, and the general value range is between 0.2 and 0.3 [30].

Select the transmission section with a small safety margin as a key section using the grid security margin. The calculation formula for the grid safety margin M_{ij} is as follows:

$$M_{ij} = 1 - \frac{P_{ij}}{P_{ij\max}} < M_{\text{set}}, \tag{19}$$

where P_{ij} is the transmission power of the line and $P_{ij\max}$ is the power transmission limit of the line. Usually, the value of M_{set} is also determined by expert experience. When the safety margin of the line is less than the threshold, it means that the line is easily affected by the power flow transfer.

3.6. Key Section Identification Algorithm. Based on the above proposed vulnerable line search method and key transmission section screening method, the complete steps of the vulnerable line identification and key transmission section search method based on PMU data and graph theory are shown in Algorithm 3.

4. Case Analysis

4.1. Vulnerable Line Identification. This paper selects an IEEE 39-bus system to verify the effectiveness of the method. System parameters are shown in reference [31]. The system has 39 bus bars and 46 transmission lines, and its structural topology is shown in Figure 6. The white points are generator nodes, and the black points are load nodes, and it is indicated that the initial power flow direction is calculated by matpower7.0. The computer configuration used in this paper is the Intel (R) core (TM) i7 with 8G memory, 128G SSD+1TB HDD. The operating system is Windows 10 64 bit, and all programs are run by using the Matlab R2020a.

According to the parameters of all nodes and branches in the IEEE 39-bus system, the PTDF value is calculated. The results of the line vulnerability assessment are shown in Figure 7. According to the above method and the data measured by PMU, the energy fluctuation probability of the line is calculated as shown in Figure 8.

The weight coefficient α of this paper is selected as 0.5. Actual values can be adjusted according to different situations. By the vulnerable line search method mentioned above, the system line vulnerability ranking is obtained. Table 1 shows the judgment indicators of the top 15 lines.

The top ten in Table 1 are the vulnerable transmission lines located in this paper. To prove the reliability of this method, the results of reference [32] and reference [33] are compared. Reference [32] uses the source load relationship and the line fault power overload to judge the vulnerability of the line from the two aspects of structure and state. In reference [33], the two types on the information on the kinetic energy of the branch potential energy are extracted for normalization, which are defined as transient vulnerability indicators. But there is no problem analysis in conjunction with the big data features of the grid in reference

Input: W, weight matrix
(1) Replace distance matrix D with matrix W.
(2) Remove the edges $k = i$, $k = j$ and $\omega_{ij} = \infty$.
(3) Use Floyd algorithm to find the shortest path and distance.
(4) Update distance matrix D and routing matrix R.
(5) If $\omega_{ij} < 0$, stop.
(6) Else if $k = n$, stop.
(7) End if
(8) End if
(9) Eliminate the same number in each element of matrix R.
(10) Traverse all elements in matrix R. If the element in R is a unit group, traverse all elements in the unit group, and generate the shortest path corresponding to the number of elements. In this way, until all the shortest paths are generated.
Output: all shortest paths

Algorithm 2: Improved Floyd algorithm.

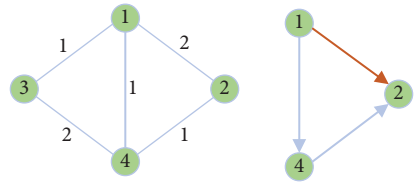

Figure 4: Minimum weight path search.

$$\begin{pmatrix} 1 & 2 & 3 & 4 \\ 1 & 2 & 3 & 4 \\ 1 & 2 & 3 & 4 \\ 1 & 2 & 3 & 4 \end{pmatrix} \Rightarrow \begin{pmatrix} 1 & (2,4) & 3 & 4 \\ (1,4) & 2 & (1,4) & 4 \\ 1 & (1,4) & 3 & (1,4) \\ 1 & 2 & (1,3) & 4 \end{pmatrix}$$

Figure 5: Routing matrix R transform.

Input: PMU data and initial power flow
(1) Construct a grid topology diagram.
(2) Calculate the PTDF and its modulus.
(3) Calculate the power transmission efficiency $\varsigma(i, j)$.
(4) Construct an observation data matrix $A(t)$ from PMU data.
(5) Calculate the total energy $E_k(t)$ and energy fluctuation probability $p_k(t)$.
(6) Calculate the comprehensive evaluation indicator Γ_{ij}.
(7) Sort the vulnerable lines.
(8) Use the improved Floyd algorithm to search flow transfer section
(9) Calculate line outage distribution factor D_{k-l}.
(10) Filter out the branch of $D_{k-l} > 0.2$.
(11) Calculate the safety margin $M_{ij.}$
(12) Filter out the branches of $M_{ij} < 0.6$.
Output: all key transmission sections.

Algorithm 3: Key transmission section search algorithm.

[32] and reference [33]. Table 2 shows the comparison results.

From the analysis of Table 2, the results of this method are basically consistent with those in reference [32] and reference [33], including seven lines 2-3, 16-17, 16–19, 3-4, 25-2, 25-26, 6–11, which indicates that this method is reasonable. Structurally, these branches are all located in the important transmission channels of the system. This paper considers line 2-3 as the most important transmission line, because it undertakes the main power transmission of generator 37 and generator 38. And also it involves the power transmission between node 3 and node 4. If overload

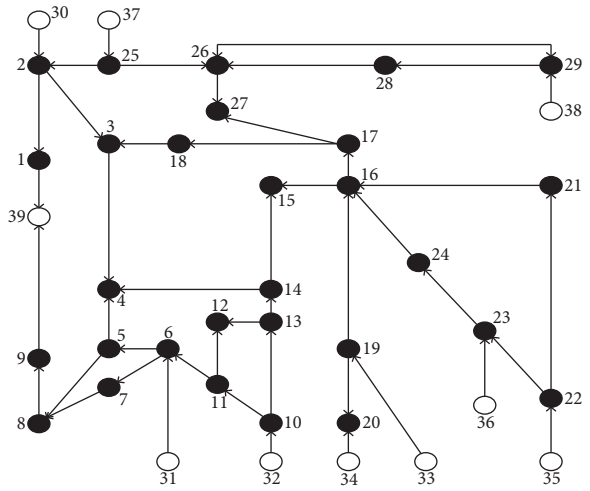

Figure 6: IEEE 39-bus system topology.

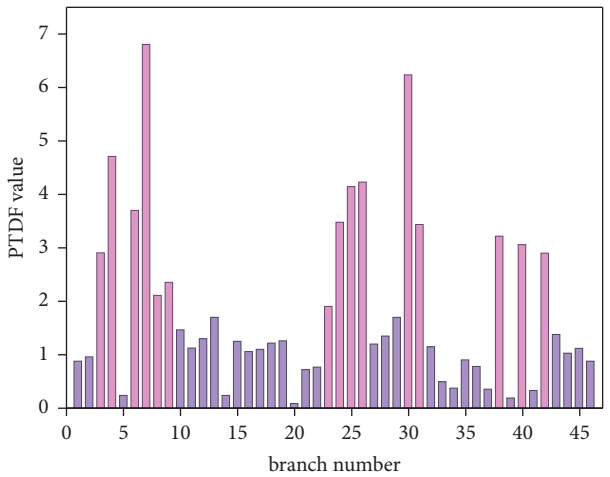

Figure 7: PTDF calculation result diagram of lines.

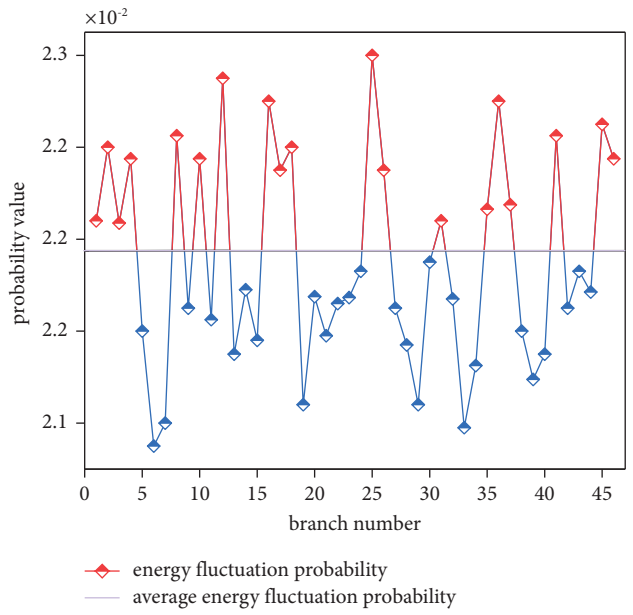

Figure 8: Distribution of the probability of energy fluctuation.

Table 1: Sorting of vulnerable lines.

Sort	Branch	$\varsigma(i, j)$	$p(k)$	Γ_{ij}
1	2-3	0.04571	0.0228	0.0343
2	6–11	0.04475	0.0227	0.0337
3	16-17	0.04392	0.0226	0.0333
4	16–19	0.04325	0.0226	0.0329
5	3-4	0.04240	0.0225	0.0325
6	25-26	0.04133	0.0225	0.0319
7	5-6	0.04095	0.02245	0.0317
8	10-11	0.04064	0.02245	0.0316
9	2–25	0.03983	0.0224	0.03111
10	10–13	0.03980	0.0224	0.0311
11	16–24	0.03745	0.02235	0.0299
12	15-16	0.03689	0.02235	0.0296
13	16–21	0.02859	0.02235	0.0255
14	4–14	0.0250	0.0223	0.0237
15	17–27	0.02230	0.0223	0.0223

Table 2: Comparison of vulnerable lines.

Sort	The method in this paper	Reference [32]	Reference [33]
1	2-3	2-3	2-3
2	6–11	6–11	16–19
3	16-17	16–19	16-17
4	16–19	25-2	15-16
5	3-4	16-17	4–14
6	25-26	13-14	25-2
7	5-6	15-16	3-4
8	10-11	26-27	25-26
9	25-2	10–13	14-15
10	10–13	16–21	16–24

protection occurs in line 2-3, generator 30 and load node 3 will be isolated, which will cause large-scale power flow transfer problem.

In addition, lines 5-6 and lines 10-11 are from the system topology. If disconnected, the normal operation of generator node 31 and node 32 will be affected. So they are judged as vulnerable lines. From the above results, the method mentioned in this paper is superior to the previous method in calculation accuracy. The uncertainty problem of the single indicator evaluation result is solved.

4.2. Key Transmission Section Search. According to the proposed method, the branch with comprehensive importance greater than 0.03 is selected to form the expected fault set. The lines are disconnected separately, and the corresponding top k least weight paths are found. In this paper, D_{set} is 0.3 and M_{set} is 0.6. Combined with the branch break distribution factor, the initial transmission section composed of lines greater than the set threshold is selected. Finally, the safety margin of the line in the section is calculated, and the key section is selected. The specific parameter results are shown in Table 3.

From Table 3, it shows that the tidal transfer sections corresponding to each vulnerable line are complex, and the branch connections in the sections are very high, which makes

Table 3: The predicted fault line corresponds to the transmission section.

Sort	Prebreak branch	Corresponding section	LOPF	Safety margin
1	2-3	25-26	0.435	0.893
		26-27	0.79	0.267
2	6–11	13-14	0.925	0.306
		10–13	0.91	0.258
		14-4	0.14	0.646
3	16-17	16-15	0.37	0.368
4	16–19	19-20	0.182	0.669
5	3-4	2-1	0.157	0.682
		1–39	0.123	0.896
6	25-26	2-3	0.856	0.196
		25-2	0.411	0.624
7	5-6	7-8	0.864	0.916
		6-7	0.37	0.353
		13-14	0.925	0.157
		10–13	0.91	0.258
		14-4	0.14	0.646
8	10-11	10–13	0.91	0.258
		13-14	0.925	0.157
		14-4	0.14	0.646
		13-12	0.23	0.795
9	2–25	25-26	0.435	0.893
		26-27	0.79	0.267
10	10–13	10-11	0.947	0.189
		11-6	0.37	0.153
		5-4	0.3	0.692
		6-5	0.921	0.624
		11-12	0.13	0.606

it easy to cause chain reaction when the fault occurs. Therefore, it is necessary to find the transmission section by identifying vulnerable lines. Using the power grid safety margin to screen out the transmission section can effectively exclude relatively safe lines and further screen key transmission sections. For example, for lines 7-8, the line outage distribution factor is large, indicating that its position in the grid structure is also relatively important. But its own safety margin is relatively large, indicating that the line-carrying capacity is strong. Therefore, it can be eliminated. For lines 19-20, the safety margin is 0.669, which is higher than the set threshold. But its power flow increment is 39.25 MW, and its correlation degree is not high in structure, which can be eliminated by the line outage distribution factor. Therefore, setting up multiple screening methods can effectively find lines with high correlation and vulnerability to the influence of tidal increments and ensure the good selection of key transmission sections.

Through the method of this paper, vulnerable power grid lines are found. The corresponding tidal transfer section is searched, and the lines in the section are further screened. Finally, it is found that the lines form the cut-off set of the power system with the vulnerable lines in the cross form the key transmission section. Table 4 shows the search results for key transmission sections. The key transmission section is represented by dotted lines, and its topology is shown in Figure 9.

Table 4: Key transmission sections.

Section number	Vulnerable line	Corresponding transmission section
1	2-3	2-3/26-27
2	6–11	6–11/13-14
3	5-6	6-5/6-7
4	10-11/10–13	10-11/10–13
5	25-26	25-26/2-3

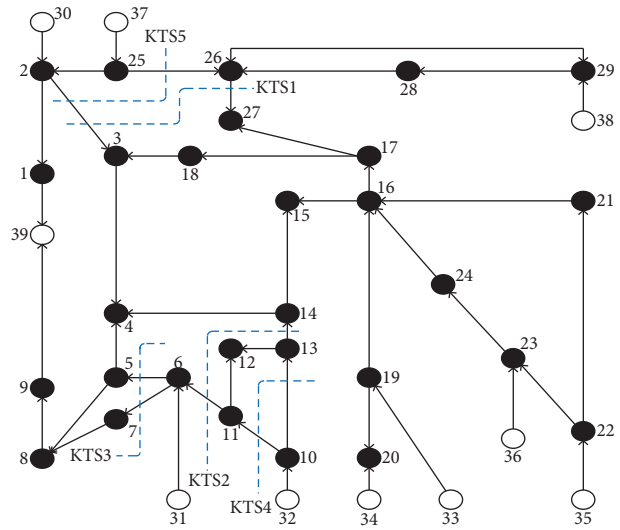

Figure 9: KTS result diagram of the IEEE 39-bus system.

From Figure 9, we can distinguish the position of each transmission section in the network. Combined with Table 4, it can be seen that disconnecting any of the lines will lead to a substantial increase in the load of other lines, resulting in serious cascading failures of the lines. In addition, when the working load of the system is large, the line in the key transmission section may also fail. Therefore, the key transmission section must be strictly monitored.

4.3. Comparison of Algorithm Calculation Time. The traditional key transmission section search method based on the graph theory generally adopts a traversal algorithm [34]. It uses the adjacency matrix of topological graph by the graph theory to identify the most serious transmission section through a simple matrix operation. But now, the new power grid structure is more complex; it will lead to inaccurate identification results, and the traversal time is also greatly increased. After fully considering the characteristics of the new power grid, the proposed method reconstructs the topology map. We set up a new shortest path search method, which significantly improves the traversal accuracy and time. The computation time of the algorithm is compared with reference [34] by performing tests on six different IEEE systems using the operating environment mentioned in Section 4.1, and the results are shown in Table 5 and Figure 10.

Table 5: Calculation time comparison of algorithms.

Test system	Algorithm of reference [34] (s)	Algorithm of this paper (s)
IEEE 9	0.056	0.032
IEEE 14	0.287	0.115
IEEE 24	13.033	0.264
IEEE 30	38.158	0.411
IEEE 39	86.365	0.689
IEEE 118	>10 min	8.735

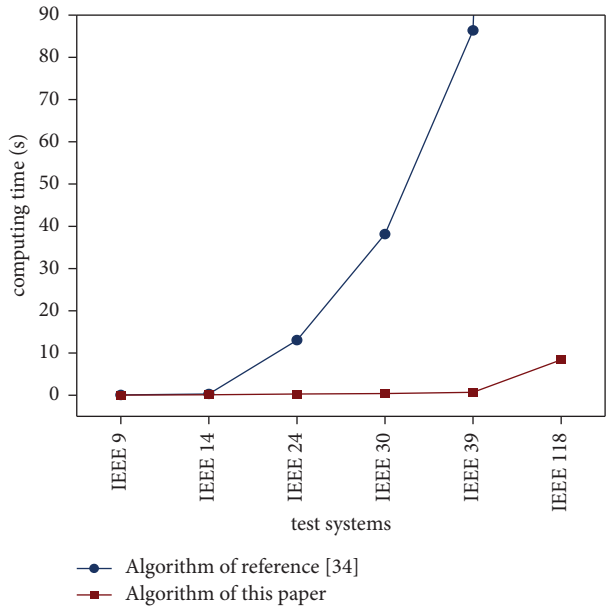

Figure 10: Calculation time comparison.

Analysis of the results in Table 5 and Figure 10 shows that the complexity of the system will greatly affect the computation time of the algorithm. For the system with more buses, the calculation time of the method proposed in reference [34] is obviously increased, and even a long unfinished calculation occurs when testing the IEEE 118-bus system. This method has obvious advantages and can quickly identify the key transmission section. The analysis of the proposed method is more comprehensive, and the improvement of the algorithm also greatly saves the calculation time. The characteristics of combining PMU also make the method more in line with online monitoring.

4.4. IEEE 14-Bus System Analysis. In order to demonstrate the applicability of the methodology of this paper, the IEEE 14-bus system is selected for the discussion, and its system structure is shown in Figure 11. The parameters of the system's initial power flow are configured by matpower 7.0 simulation tool.

Based on the methodology mentioned in Section 2 and Section 3 of this paper, the results of the identified parameters of the vulnerable transmission line are obtained as shown in Figure 12 and Figure 13, and the detailed results are presented in Table 6.

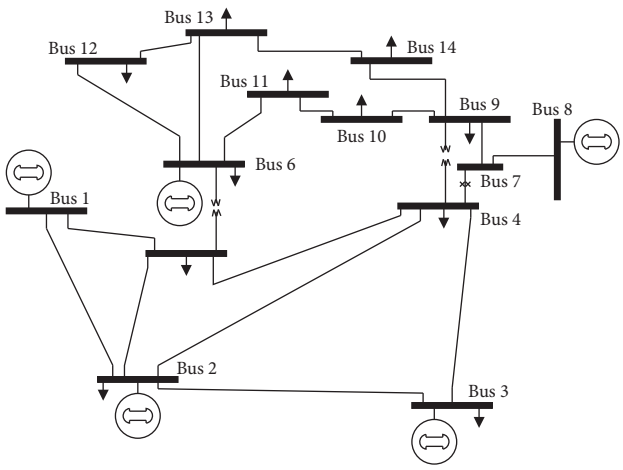

Figure 11: IEEE 14-bus system wiring diagram.

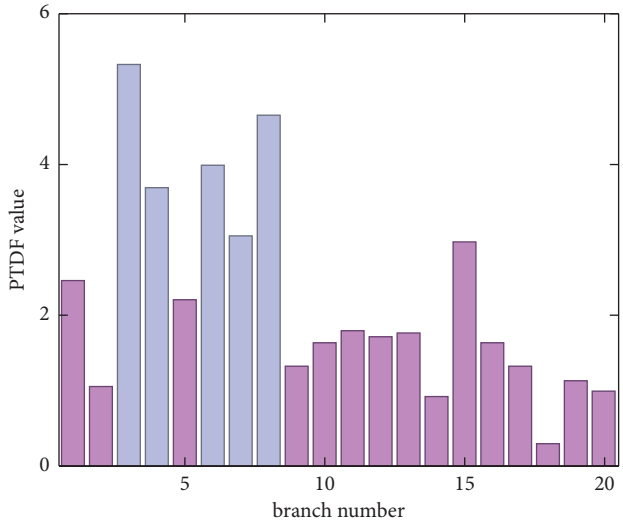

Figure 12: IEEE 14-bus system PTDF calculation results.

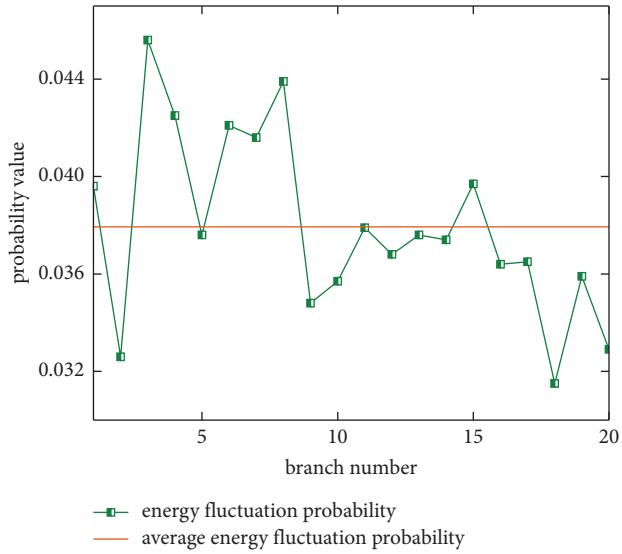

Figure 13: IEEE 14-bus system energy fluctuation probability distribution.

Table 6: IEEE 14-bus system vulnerable line identification results.

Sort	Branch	$\eta(i,j)$	$p(k)$	Γ_{ij}
1	2-3	0.0519	0.0456	0.04875
2	4–7	0.0498	0.0439	0.04685
3	3-4	0.0472	0.0421	0.04465
4	2–4	0.0461	0.0425	0.0443
5	5-4	0.0453	0.0416	0.04345

Table 7: IEEE 14-bus system vulnerable lines and its transmission section.

Sort	Prebreak branch	Corresponding section	LOPF	Safety margin
1	2-3	2–4	0.776	0.428
		2–5	0.895	0.439
2	4–7	4–9	0.668	0.883
		9-10	0.215	0.725
3	3-4	2-3	0.492	0.716
4	2–4	5-4	0.618	0.362
		2-3	0.492	0.716
5	5-4	2–4	0.776	0.428
		2-3	0.492	0.716
		1–5	0.526	0.625

Table 8: IEEE 14-bus system key transmission sections.

Section number	Vulnerable line	Corresponding transmission section
1	2-3	2–4/2–5
2	2–4	5-4
3	5-4	2–4

According to the identification results of vulnerable transmission lines, their corresponding transmission sections and related parameters are calculated as shown in Table 7.

Based on the results of Table 7, the results of key transmission cross sections are screened with reference to (18) and (19), which are shown in Table 8.

In summary, it can be seen that the method of this paper can search the vulnerable transmission lines with their key transmission cross sections in different systems, which indicates that the method of this paper has a head of certain universality.

5. Conclusion

The structure of interconnected power systems is becoming more and more complex, and accurately locating the vulnerable transmission lines and their corresponding critical transmission sections can be of great help in preventing chain failures in power system. In this paper, a multilevel method for identifying key transmission sections in power systems is proposed, and the following conclusions are obtained.

(1) The discrimination of vulnerable lines in the power system needs to fully consider the network topology and the carrying capacity of the lines themselves. Therefore, this paper proposes the first layer method: Constructing the grid topology map from the perspective of spatial visualization of PMU data. On this basis, two indicators, power transmission efficiency and energy fluctuation probability, are proposed to comprehensively assess the line vulnerability. The comprehensive indicators fully consider the two factors, making the results more accurate.

(2) Transmission section is a collection of lines affected by chain faults caused by current transfer after the failure of vulnerable lines. In this regard, the second layer method of this paper is as follows: For the previous transmission cross-section mis-selection and leakage detection and long time-consuming problems, this paper improves the Floyd algorithm, which greatly improves the computational efficiency and algorithmic accuracy and realizes the precise positioning of the transmission cross-section corresponding to the vulnerable lines.

(3) The key transmission section is the set of lines that should receive the most focused attention in the tidal shift section. In this paper, the third layer of the method: selecting the key transmission section based on two indicators: line tidal current distribution factor and line safety margin, which can give more accurate results.

The construction method of the grid topology diagram proposed in this paper has more advantages, and it can directly obtain the corresponding parameters, which can be used as a reference for the analysis of line power flow. The vulnerable transmission lines and their key transmission sections in this paper have certain significance for the analysis of power grid fault types and the transmission capacity of lines. In the future, a deep learning method can be introduced into the search of transmission sections to meet the section identification under multifault types.

Data Availability

Data used to support the findings of this study are made available upon reasonable request to the corresponding author.

Conflicts of Interest

The authors declare that there no conflicts of interest.

Acknowledgments

The work was supported by the Shandong University Key Laboratory of Power System Intelligent Dispatch and Control, Ministry of Education; Pyramid Talent Training Project of Beijing University of Civil Engineering and Architecture (JDYC20200324); Cultivation project Funds for Beijing University of Civil Engineering and Architecture under Grant (X23050); and National Natural Science Foundation of China (51407201).

References

[1] V. Rampurkar, P. Pentayya, H. A. Mangalvedekar, and F. Kazi, "Cascading failure analysis for Indian power grid," *IEEE Transactions on Smart Grid*, vol. 7, no. 4, pp. 1951–1960, 2016.

[2] Y. Liu, "Analysis on and inspiration of the "9.13" islanding and outage of Brazilian remote northwest power grid," *Pro. CSEE*, vol. 38, no. 11, pp. 3204–3213, 2018.

[3] Y. Susuki and I. Mezic, "Nonlinear koopman modes and power system stability assessment without models," *IEEE Transactions on Power Systems*, vol. 29, no. 2, pp. 899–907, 2014.

[4] M. Honarvar Nazari, Z. Costello, M. J. Feizollahi, S. Grijalva, and M. Egerstedt, "Distributed frequency control of prosumer-based electric energy systems," *IEEE Transactions on Power Systems*, vol. 29, no. 6, pp. 2934–2942, 2014.

[5] J. Kim, J. A. Bucklew, and I. Dobson, "Splitting method for speedy simulation of cascading blackouts," *IEEE Transactions on Power Systems*, vol. 28, no. 3, pp. 3010–3017, 2013.

[6] I. Dobson, B. A. Carreras, and D. E. Newman, "How many occurrences of rare blackout events are needed to estimate event probability," *IEEE Transactions on Power Systems*, vol. 28, no. 3, pp. 3509-3510, 2013.

[7] X. Zhang and S. Grijalva, "Decentralized total transfer capability evaluation using domain decomposition methods," *IEEE Transactions on Power Systems*, vol. 31, no. 5, pp. 3349–3357, 2016.

[8] L. Min and A. Abur, "Total transfer capability computation for multi-area power systems," *IEEE Transactions on Power Systems*, vol. 21, no. 3, pp. 1141–1147, 2006.

[9] S. Grijalva, P. W. Sauer, and J. D. Weber, "Enhancement of linear ATC calculations by the incorporation of reactive power flows," *IEEE Transactions on Power Systems*, vol. 18, no. 2, pp. 619–624, 2003.

[10] R. Yao, S. W. Huang, K. Sun et al., "Risk assessment of multi-timescale cascading outages based on Markovian tree search," *IEEE Transactions on Power Systems*, vol. 32, no. 4, pp. 2887–2900, 2017.

[11] Z. Chao, M. Tian, and M. S. Ying, "Transient stability identification and emergency control based on the convex characteristic of the key branch's disturbed trajectory," *Proc CSEE*, vol. 36, no. 10, pp. 2600–2607, 2016.

[12] Z. Ting, D. Y. Chen, X. Wei, R. X. Cheng, and L. Lin, "Online identification method of a key transmission section considering multi-faults," *Power System Protection Control*, vol. 49, no. 4, pp. 45–53, 2021.

[13] K. Wang, B. Zhang, Z. Zhang, X. G. Yin, and B. Wang, "An electrical betweenness approach for vulnerability assessment of power grids considering the capacity of generators and load," *Physica A: Statistical Mechanics and Its Applications*, vol. 390, no. 23-24, pp. 4692–4701, 2011.

[14] F. Wenli, L. Zhigang, H. Ping, and M. Shengwei, "Cascading failure model in power grids using the complex network theory," *IET Generation, Transmission & Distribution*, vol. 10, no. 15, pp. 3940–3949, 2016.

[15] W. L. Fan, X. M. Zhang, S. W. Mei, and S. W. Huang, "Vulnerable transmission line identification considering depth of *K*-shell decomposition in complex grids," *IET Generation, Transmission & Distribution*, vol. 12, no. 5, pp. 1137–1144, 2018.

[16] X. Wei, J. Zhao, T. Huang, and E. Bompard, "A novel cascading faults graph based transmission network vulnerability assessment method," *IEEE Transactions on Power Systems*, vol. 33, no. 3, pp. 2995–3000, 2018.

[17] Z. Lin, F. Wen, H. Wang, G. Lin, T. Mo, and X. Ye, "CRITIC-based node importance evaluation in skeleton-network reconfiguration of power grids," *IEEE Transactions on Circuits and Systems II: Express Briefs*, vol. 65, no. 2, pp. 206–210, 2018.

[18] Q. Zhang, W. Fan, Z. Qiu, Z. Liu, and J. Zhang, "A new identification approach of power system vulnerable lines based on weighed H-index," *IEEE Access*, vol. 7, pp. 121421–121431, 2019.

[19] H. J. Xian, H. M. Xiao, D. Y. Feng, W. Yi, and B. G. Quan, "Weak transmission sections fast searching and identification method in online stability assessment," in *Proceedings of the International Conference on Information Science Electronics and Electrical Engineering*, pp. 1918–1922, Sapporo, Japan, April 2014.

[20] B. Xue and D. J. Dong, "Typical transmission section searching method considering geographical attributes for large power grids," in *Proceedings of the 14th IET International Conference on AC and DC Power Transmission*, pp. 3051–3055, Chengdu, China, June 2018.

[21] L. Ying, H. Jinxiu, W. Yiyu et al., "Key transmission section identification method for large scale power grid with multiple faults," in *Proceedings of the International Conference on Power System Technology (POWERCON)*, pp. 4161–4168, Guangzhou, China, November 2018.

[22] B. Liu, Z. Li, X. Chen, Y. Huang, and X. Liu, "Recognition and vulnerability analysis of key nodes in power grid based on complex network centrality," *IEEE Transactions on Circuits and Systems II: Express Briefs*, vol. 65, no. 3, pp. 346–350, 2018.

[23] P. Hu and W. L. Fan, "Mitigation strategy against cascading failures considering vulnerable transmission line in power grid," *Physica A*, vol. 540, 2019.

[24] P. D. Jong, C. Sprenger, and F. Veen, "On extreme values of Moran's I and Geary's c," *Geographical Analysis*, vol. 16, no. 1, pp. 17–24, 2010.

[25] D. Borcard and P. Legendre, "All-scale spatial analysis of ecological data by means of principal coordinates of neighbour matrices," *Ecological Modelling*, vol. 153, no. 1-2, pp. 51–68, 2002.

[26] W. Luo, M. C. Taylor, and S. R. Parker, "A comparison of spatial interpolation methods to estimate continuous wind speed surfaces using irregularly distributed data from England and Wales," *International Journal of Climatology*, vol. 28, no. 7, pp. 947–959, 2008.

[27] N. S.-N. Lam, "Spatial interpolation methods: a review," *The American Cartographer*, vol. 10, no. 2, pp. 129–150, 1983.

[28] S. Zhang, M. Yu, J. Hu, J. Sun, J. Wei, and Y. Wu, "Research on vulnerable line identification based on PMU data and graph theory," in *Proceedings of the Power System and Green Energy Conference (PSGEC)*, pp. 853–858, Shanghai, China, August 2022.

[29] M. Giuntoli, V. Biagini, and K. Schönleber, "Novel formulation of PTDF and LODF matrices for security constrained optimal power flow for hybrid AC and DC grids," in *Proceedings of the IEEE PES Innovative Smart Grid Technologies Europe (ISGT-Europe)*, pp. 1–5, Bucharest, Romania, September 2019.

[30] D. Zhang, N. Wang, H. Yang et al., "Fast search algorithm for key transmission sections based on topology converging adjacency matrix," *IEEE Access*, vol. 8, pp. 108235–108246, 2020.

[31] Iee, "23st model," http://www2.iee.or.jp/ver2/pes/23st_model/english/index.html.
[32] L. L. Min, L. J. Yong, and W. Z. Bo, "Transmission line vulnerability assessment based on synergetic effect analysis," *Electric Power Automatical Equipment*, vol. 36, no. 5, pp. 30–37, 2016.
[33] L. Y. Bo, L. J. Yong, and W. M. Kun, "Fast assessment method for transient vulnerability of transmission lines based on kinetic energy injection betweenness," *Proc CSEE*, vol. 31, no. 13, pp. 40–47, 2011.
[34] Z. D. Cai, Z. B. Hui, Y. Feng, W. L. Yong, Z. B. Guo, and Z. Y. Shu, "Fast search of transmission section based on graph theory," *Proc CSEE*, vol. 26, no. 12, pp. 32–38, 2006.